

Defect diffusion and closed-time distributions for ionic channels in cell membranes

C. A. Condat

Fakultät für Physik, Universität Konstanz, Postfach 5560, D-7750 Konstanz 1, West Germany

(Received 19 September 1988)

The ionic channels associated with proteins embedded in cell membranes often show a fluctuating behavior between open and closed states. A feature commonly observed is the long-time tail in the distribution $f(t)$ of closed-state durations. A generalization of a defect-diffusion model recently proposed to explain this behavior is solved analytically for a one-dimensional geometry. The analysis involves the solution of a target annihilation problem with a finite annihilation rate for the target hit by a walker. While at short times $f(t)$ may decay exponentially, at long times the solution is dominated either by a power law or a stretched exponential, depending on the initial defect configuration. The predictions of the model are shown to be in agreement with experimental data.

I. INTRODUCTION

In the last few years, biophysicists have devoted a considerable amount of work to the recording and analysis of ionic currents flowing through cell membranes.^{1,2} These currents, which are associated with proteins imbedded in the membrane, frequently show a fluctuating behavior, characterized by oscillations between open (conducting) and closed (nonconducting) states.

The introduction by Neher and Sakmann of the patch-clamp method made possible the detailed analysis of the conducting properties of single ionic channels.^{3,4} At present a large body of experimental data related to these channels has been collected. Of particular interest is the study of the distribution $f(t)$ of closed-state durations. This distribution often shows a long-time tail, and it has been customary to fit it with a superposition of exponentials. These exponentials are usually associated with the existence of a few inner conformational states of the channel, the transitions among which are assumed to be Markovian.^{1,2,5}

It has recently been pointed out, however, that in many cases a sum of exponentials may not be the most suitable way of fitting the data.⁶⁻⁹ Liebovitch *et al.* assumed that the kinetic rate constant associated with the transition from the closed state to the open state has a power-law dependence on the time. This assumption, which would be consistent with a fractal interpretation of the protein dynamics, implies that $f(t)$ is given by Kohlrausch's stretched exponential function. The stretched exponential form permitted a good fit to the data obtained by the same group for a channel in rabbit corneal endothelium.⁶ Millhauser *et al.*, on the other hand, assumed that the kinetics of the gating is Markovian, but suggested that the proteins have a large number of states of similar energy.⁷ This permits the interpretation of gating as a diffusion process, leading to a power-law dependence for $f(t)$.

Läuger's defect-diffusion model, which provides a specific physical process to account for the channel gating, is especially appealing.⁸ In a previous communica-

tion we gave an analytical solution to a generalization of its one-dimensional version, showing how it correctly describes an assortment of experimental data.⁹ The objective of this paper is to present the detailed derivation of the solution to the extended Läuger model. The solution involves the analysis of the properties of a random walk with an absorbing boundary of arbitrary strength. In our generalization we also include a background of randomly distributed defects that compete with Läuger's original defect to annihilate the target (i.e., to reopen the channel). The many-defect aspects of the problem are closely related to Glarum's model of molecular relaxation in viscous liquids.¹⁰

The Glarum model has been applied to the study of dielectric relaxation^{10,11} and stress relaxation in viscous liquids.¹² In general terms, it is of interest in the theory of target annihilation by random walkers.^{13,14} It is usually assumed that the relaxation occurs instantaneously when any of the diffusing defects reaches the target. Under this assumption, the solution to Glarum's model was given by Bordewijk.¹¹ The model was later solved by Shlesinger and Montroll in the framework of the continuous-time random walk.¹⁵ These authors showed that, while an exponential waiting-time distribution leads to Bordewijk's results, a power-law distribution always leads to the Williams-Watts fractional exponential.¹⁶

In order to find the solution to our extended version of Läuger's model, we must solve a many-walker target-relaxation (or annihilation) problem. In this problem the probability of relaxation of the target upon an encounter with a defect is finite, so that defect and target may survive one or more encounters. For the sake of clarity in the presentation, and because we believe that some of the intermediate results may be of use outside the biophysical community, we present first the one- and many-walker aspects of the calculation (in Secs. II and III, respectively); the description of Läuger's model is left to Sec. IV, where we also give its solution and analyze some of the available data for ionic channels. These are found to give strong support to the applicability of the model.

II. SINGLE-DEFECT KINETICS

A. Solution to the master equation

Let us describe the kinetics of a single defect which starts at $t=0$ from site s on a semi-infinite one-dimensional lattice. (See Fig. 1.) The defect is allowed to perform a symmetric, one-step random walk on the lattice; upon arriving at the site $s=1$, it can leave the lattice (“jump into limbo”) with a probability γ . The defect kinetics can then be described by a master equation for the continuous-time random walk:

$$\dot{p}_{ns}(\gamma, t) = p_{n+1,s} + p_{n-1,s} - 2p_{ns} \quad (n > 1) \quad (2.1a)$$

and

$$\dot{p}_{1s}(\gamma, t) = p_{2s} - (1 + \gamma)p_{1s}. \quad (2.1b)$$

Here we have defined $p_{ns}(\gamma, t)$ as the probability that a defect at site s at time $t=0$ is at site n at time t , given the absorption rate γ at the boundary.

The probability that the defect has been absorbed by time t is given by

$$P_s^*(\gamma, t) = 1 - P_s(\gamma, t), \quad (2.2)$$

where $P_s(\gamma, t)$ is the probability that the defect is still on the lattice at time t , i.e.,

$$P_s(\gamma, t) = \sum_{n=1}^{\infty} p_{ns}(\gamma, t). \quad (2.3)$$

$P_s(\gamma, t)$ and $P_s^*(\gamma, t)$ can be referred to as the “survival probability” and the “limbo occupation probability,” respectively.

Following van Kampen and Oppenheim^{17,18} we next solve Eqs. (2.1) exactly. The solution $p_{ns}(\gamma, t)$ can be expressed as a superposition of normal modes having the form

$$e^{-\lambda t} \phi_n(\lambda) = e^{-\lambda t} (c_1 Z_1^n + c_2 Z_2^n), \quad (2.4)$$

where Z_1 and Z_2 solve the characteristic equation

$$Z + Z^{-1} + \lambda - 2 = 0. \quad (2.5)$$

We must require that λ be non-negative and that the solution not grow without limits as $n \rightarrow \infty$. If $0 < \lambda < 4$, Z_1 and Z_2 are the complex conjugates of each other,

$$Z_2^* = Z_1 = e^{iq} \quad (0 \leq q \leq \pi), \quad (2.6)$$

with $\lambda = 2(1 - \cos q)$. The coefficients c_1 and c_2 in Eq. (2.4) are not independent.

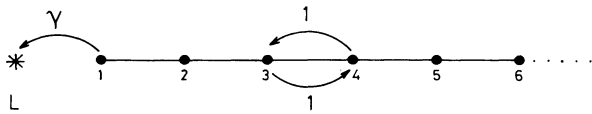


FIG. 1. Random walk on a semi-infinite chain with an absorbing boundary. The absorbed walker may be visualized as jumping into a limbo state L .

Using Eq. (2.1b) we find

$$\frac{c_1}{c_2} = -\frac{1 + (\gamma - 1)e^{-iq}}{1 + (\gamma - 1)e^{iq}} \equiv S(q). \quad (2.7)$$

Although for $0 \leq \gamma \leq 2$, $S(q)$ is analytical in the upper half q plane, for $\gamma > 2$ it has simple poles located at

$$q_j = (2j + 1)\pi + i \ln(\gamma - 1), \quad (2.8)$$

with j being an integer.

If $\lambda > 4$, Eq. (2.5) has two solutions. However, it is easy to see using the finiteness requirements that no acceptable real solution is possible if $\gamma < 2$. Furthermore, for each $\gamma > 2$, there is a single allowed value of λ , $\tilde{\lambda} = \gamma^2(\gamma - 1)^{-1}$, and the corresponding mode is given by

$$e^{-\tilde{\lambda} t} \tilde{\phi}_n = c(\gamma) e^{-\tilde{\lambda} t} (1 - \gamma)^{-n}. \quad (2.9)$$

Thus the spectrum consists of a continuum of values of λ (or q), to which we must add an isolated point if $\gamma > 2$. The completeness is verified (and the normalization obtained) by proving the closure relation,

$$\int_0^\pi \phi_n(q) \phi_s(q) dq + \theta(\gamma - 2) \tilde{\phi}_n \tilde{\phi}_s = \delta_{ns}, \quad (2.10)$$

where $\theta(x)$ is the step function. After a simple transformation, the integral over q can be carried out using the contour shown in Fig. 2.^{17,18} The contribution of the vertical branches cancels due to the periodicity of the integrand. If $\gamma > 2$ the contribution of the isolated real solution cancels with the residue at the enclosed pole. (Note that the residue vanishes if $\gamma = 2$.) Finally, the solution to the master equation is obtained if we use the initial condition $p_{ns}(\gamma, t=0) = \delta_{ns}$ to determine the coefficients in the normal-mode sum. After some algebra we find

$$p_{ns}(\gamma, t) = \int_0^\pi \phi_n(q) \phi_s(q) e^{-\lambda(q)t} dq + \theta(\gamma - 2) e^{-\tilde{\lambda} t} \tilde{\phi}_n \tilde{\phi}_s, \quad (2.11)$$

where

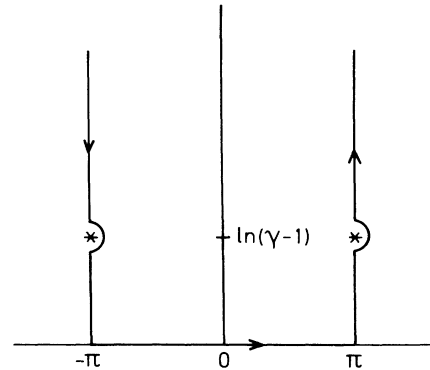


FIG. 2. Complex q -plane contour used for the evaluation of the integral in Eq. (2.10). The simple poles appear if $\gamma \geq 2$.

$$\phi_n(q) = \left[\frac{2}{\pi} \right]^{1/2} \frac{\sin(qn) + (\gamma - 1)\sin[q(n-1)]}{[1 + 2(\gamma - 1)\cos q + (\gamma - 1)^2]^{1/2}}, \quad (2.12a)$$

$$\lambda(q) = 2(1 - \cos q), \quad (2.12b)$$

and

$$\tilde{\phi}_n = \frac{(-1)^n [\gamma(\gamma - 2)]^{1/2}}{(\gamma - 1)^n}. \quad (2.12c)$$

We digress for a moment to remark that the problem of obtaining the solutions $\phi_n(q)$ is equivalent to that of solving the stationary Schrödinger equation for an exciton in a semi-infinite chain.¹⁹ The corresponding solution for the exciton can be obtained from Eqs. (2.12) through the transformation

$$(2 - \lambda) \rightarrow (E - \alpha)\beta^{-1}, \quad 1 - \gamma \rightarrow \tilde{Q},$$

where α is the diagonal matrix element of the exciton Hamiltonian, β the nearest-neighbor interaction, E the Schrödinger equation eigenvalue, and \tilde{Q} measures the strength of the surface relaxation. However, the solution to the time-dependent Schrödinger equation leads to a complex time-evolution factor, $\exp(-2it \cos q)$. As a consequence, the exciton site-occupation probabilities are expressed in terms of the Bessel functions $J_n(2t)$ instead of the modified Bessel functions $I_n(2t)$ that will be seen to appear in the solution to the master Eq. (2.1).

The denominator in Eq. (2.11) can be expanded in terms of Chebyshev functions:

$$\frac{1}{1 - 2\omega \cos q + \omega^2} = \sum_{k=0}^{\infty} \frac{\sin[(k+1)q]}{\sin q} \omega^k \quad (2.13)$$

($|\omega| < 1$). Using this expansion, $p_{ns}(\gamma, t)$ may be expressed as a series of modified Bessel functions (cf. Ref. 19),

$$p_{ns}(\gamma < 2, t) = e^{-2t} \left[I_{n-s}(2t) - I_{n+s}(2t) + \frac{1}{t} \sum_{k=1}^{\infty} (k+n+s-1) I_{k+n+s-1}(2t) \times (1-\gamma)^k \right], \quad (2.14)$$

and

$$p_{ns}(\gamma > 2, t) = e^{-2t} \left[I_{n-s}(2t) - I_{n+s-2}(2t) + \frac{1}{t} \sum_{k=1}^{\infty} (k-n-s+1) I_{k-n-s+1}(2t) \times (1-\gamma)^{-k} \right] + \gamma(\gamma-2)(1-\gamma)^{-n-s} g(t), \quad (2.15)$$

with

$$g(t) = \exp[-\gamma^2 t / (\gamma - 1)]. \quad (2.16)$$

These expansions can be truncated to provide useful approximate results in the cases $|\gamma - 1| \ll 1$ and $\gamma \gg 1$.

If $\gamma = 2$, Eq. (2.11) reduces to

$$p_{ns}(2, t) = e^{-2t} [I_{n-s}(2t) - I_{n+s-1}(2t)]. \quad (2.17)$$

In the absence of absorption (i.e., for a reflecting boundary), it follows that

$$p_{ns}(0, t) = e^{-2t} [I_{n-s}(2t) + I_{n+s-1}(2t)]. \quad (2.18)$$

If $\gamma = 0$ or $\gamma = 1$ these results can be immediately obtained using the method of images.²⁰

It should be noted that the contribution of the “isolated” solution, i.e., of the discrete mode, can be expressed as a series of Bessel functions. Using the generating function, we find

$$g(t) = e^{-2t} \sum_{k=-\infty}^{\infty} (1-\gamma)^{-k} I_k(2t). \quad (2.19)$$

A remarkable property of the solutions (2.14) and (2.15) is that, notwithstanding the different forms of the Chebyshev expansions for $\gamma < 2$ and $\gamma > 2$, the right-hand side of Eq. (2.15) can be transformed into that of Eq. (2.14): Because of the addition of the discrete mode a single formal expression is valid over the entire γ range. The proof, which makes use of Eq. (2.19) and the recurrence relation for the Bessel functions, is straightforward.

In accordance with Eq. (2.3), the survival probability $P_s(\gamma, t)$ for a defect that started its walk from site s at $t=0$ is obtained by summing $p_{ns}(\gamma, t)$ over all n . The probability density $f_s(\gamma, t)$ that this defect is absorbed at time t is then given by the derivative

$$f_s(\gamma, t) = -\frac{\partial P_s(\gamma, t)}{\partial t}. \quad (2.20a)$$

The following alternative expression is also useful:

$$f_s(\gamma, t) = \gamma p_{1s}(\gamma, t). \quad (2.20b)$$

In case only the initial distribution function is specified, the probability $p_n(\gamma, t)$ that the defect is at site n at time t can be written as

$$p_n(\gamma, t) = \sum_{s=1}^{\infty} a_s p_{ns}(\gamma, t), \quad (2.21)$$

where a_s is the probability that the defect started the walk from site s .

B. A special case: $s=1$

As an important example, we next analyze the case $s=1$: the defect starts its random walk at $t=0$ from the first lattice site. The site-occupation probabilities have the form

$$p_{n1}(0,t) = e^{-2t}[I_{n-1}(2t) + I_n(2t)] , \quad (2.22a)$$

$$p_{n1}(0 < \gamma < 2, t) = t^{-1} e^{-2t} \left[n I_n(2t) + \sum_{k=1}^{\infty} (k+n) I_{k+n}(2t) (1-\gamma)^k \right] , \quad (2.22b)$$

$$p_{n1}(1, t) = t^{-1} e^{-2t} n I_n(2t) , \quad (2.22c)$$

$$p_{n1}(2, t) = e^{-2t} [I_{n-1}(2t) - I_n(2t)] , \quad (2.22d)$$

and

$$p_{n1}(\gamma > 2, t) = t^{-1} e^{-2t} \sum_{k=1}^{\infty} (k-n) I_{k-n}(2t) (1-\gamma)^{-k} + (-1)^{n+1} \gamma (\gamma-2) (\gamma-1)^{-(n+1)} g(t) . \quad (2.22e)$$

Because of the result described in the paragraph following Eq. (2.19), Eq. (2.22b) is actually valid for all values of γ . Nevertheless, since Eq. (2.22b) is not appropriate for a high- γ truncation, we also give explicitly the form (2.22e).

Using Eqs. (2.3) and (2.22) we can calculate the average displacement of a *surviving walker*

$$\langle x(\gamma, t) \rangle = P_1^{-1}(\gamma, t) \sum_{n=1}^{\infty} n p_{n1}(\gamma, t) . \quad (2.23)$$

It can be seen that the usual long-time behavior obtains $\langle x(t \rightarrow \infty) \rangle \sim t^{1/2}$.

From Eqs. (2.16) and (2.22e) it is clear that the solutions $\bar{\phi}_n$ is important only at short times and close to the boundary. In that sense we can refer to it (somewhat loosely) as a "surface" state. In Figs. 3 and 4 we plot the occupation probabilities for the first few lattices sites in the cases $\gamma=1$ and $\gamma=30$, respectively. The higher

boundary absorption for $\gamma=30$ translates into a sharpening of the maxima, which are also shifted towards shorter times. In Fig. 4 we can see how crucial is the contribution of $\bar{\phi}_n$ at short times, if $\gamma > 2$ and n is small. The probability density for absorption is plotted in Fig. 5 for several values of γ . Note that, in the curves for $\gamma=10$ and $\gamma=30$, the "surface" state accounts for most of the high absorption occurring at short times.

At the shortest times the site-occupation probabilities grow as

$$p_{n1} \sim \frac{t^{n-1}}{(n-1)!} \quad (n > 1) . \quad (2.24)$$

As it should be expected, the farther a site is from the origin, the slower the growth of its occupation probability.

It is convenient to have the survival probability expressed as an integral; from Eqs. (2.11) and (2.12),

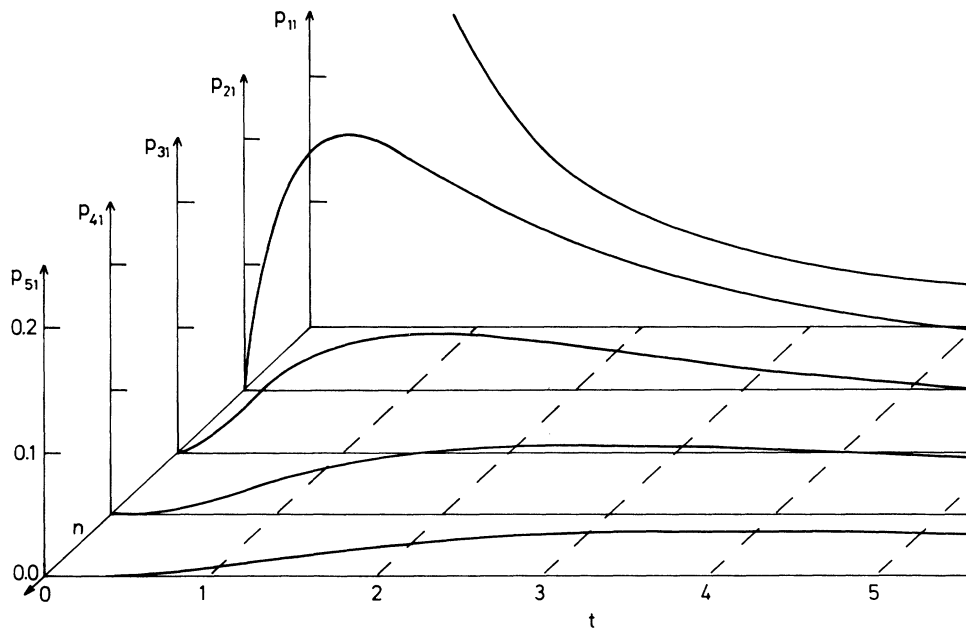


FIG. 3. Occupation probabilities for the sites 1 to 5 in the case $\gamma=1$. The defect started its random walk from site $s=1$ at $t=0$.

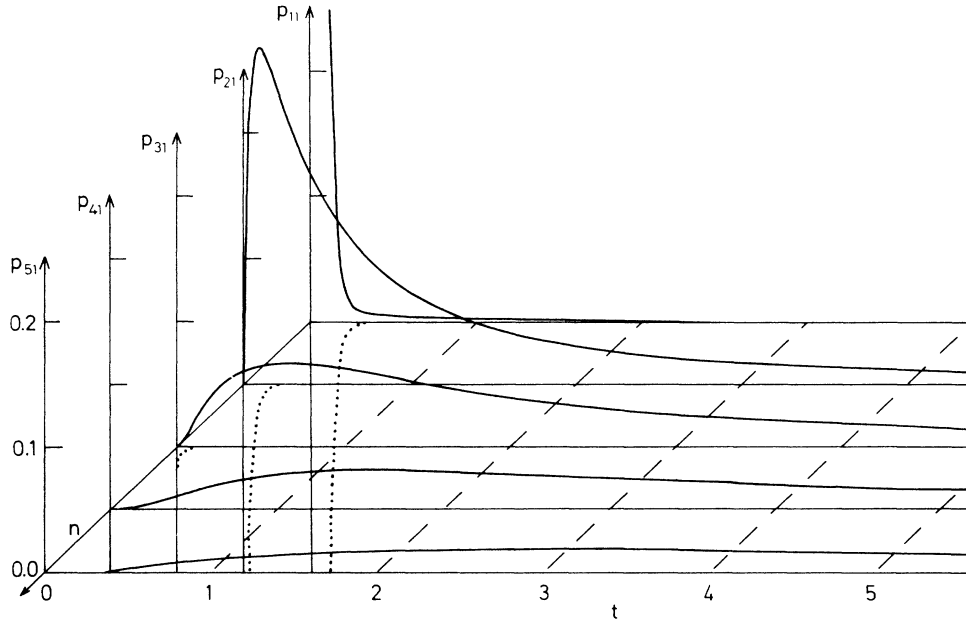


FIG. 4. Same as in Fig. 3, but for $\gamma=30$. The dotted lines represent $(-1)^n$ times the contribution of the surface state, essential at and only at short times.

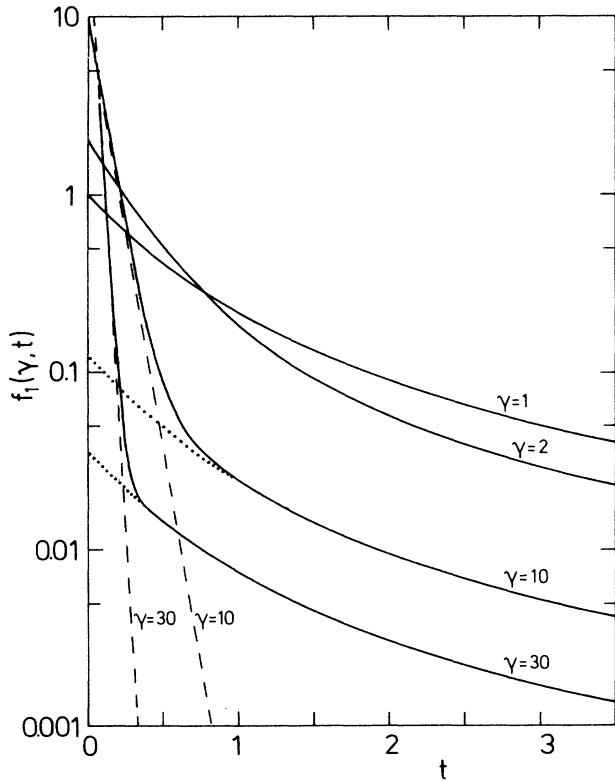


FIG. 5. Probability density f_1 for defect absorption as a function of time for the indicated values of γ . In the $\gamma > 2$ cases the dotted line represents the contribution of the continuum states, the dashed lines that of the surface state.

$$P_1(\gamma, t) = \frac{\gamma}{\pi} \int_0^\pi h(q)(1 + \cos q)e^{-2t(1 - \cos q)} dq + (\gamma - 2)(\gamma - 1)^{-1}g(t)\theta(\gamma - 2), \quad (2.25)$$

where

$$h(q) = [1 + 2(\gamma - 1)\cos q + (\gamma - 1)^2]^{-1}. \quad (2.26)$$

The probability density for absorption is equal to

$$f_1(\gamma, t) = \frac{2\gamma}{\pi} \int_0^\pi h(q)\sin^2 q e^{-2t(1 - \cos q)} dq + \gamma^2(\gamma - 2)(\gamma - 1)^{-2}g(t)\theta(\gamma - 2). \quad (2.27)$$

Alternatively, using Eqs. (2.20b) and (2.22),

$$f_1(\gamma < 2, t) = \gamma t^{-1} e^{-2t} \sum_{k=1}^\infty k I_k(2t)(1 - \gamma)^{k-1}, \quad (2.28a)$$

and

$$f_1(\gamma > 2, t) = \gamma t^{-1} e^{-2t} \sum_{k=1}^\infty k I_k(2t)(1 - \gamma)^{-(k+1)} + \gamma^2(\gamma - 2)(\gamma - 1)^{-2}g(t). \quad (2.28b)$$

The forms for $\gamma = 1$ and $\gamma = 2$ are again very simple,

$$P_1(1, t) = e^{-2t}[I_0(2t) + I_1(2t)], \quad (2.29a)$$

$$f_1(1, t) = t^{-1} e^{-2t} I_1(2t), \quad (2.29b)$$

$$P_1(2, t) = e^{-2t} I_0(2t), \quad (2.30a)$$

$$f_1(2, t) = 2e^{-2t}[I_0(2t) - I_1(2t)]. \quad (2.30b)$$

Obviously, $P_1(0, t) = 1$ and $f_1(0, t) = 0$.

The initial value for the probability density is

$f_1(\gamma, 0) = \gamma$, a special case of Eq. (2.20b). It is also easy to verify that the "limbo" state is empty at $t=0$: $P_1^*(\gamma, 0) = 1 - P_1(\gamma, 0) = 0$.

The integral in Eq. (2.27) may be evaluated by expanding the integrand as a power series in t . The resulting coefficients are, however, complicated and the general expression is not very illuminating. Let us only write down the first terms in the expansion to show the relative sizes of the continuum and discrete modes at short times. If $\gamma > 2$,

$$f_1(\gamma, t) = \gamma(\gamma - 1)^{-2} \{ [\gamma(\gamma - 2) + 1] - [\gamma^3(\gamma - 2) + (2\gamma - 1)] \times (\gamma - 1)^{-1} t + \dots \}. \quad (2.31)$$

Here the first (second) term inside each of the square brackets represents the contribution of the discrete (continuum) mode(s). The discrete mode dominates completely the short-time behavior when γ is large. After a simple rearrangement, Eq. (2.31) can be written as

$$f_1(\gamma, t) = \gamma [1 - (\gamma + 1)t + (\gamma^2 + 2\gamma + 2)2^{-1}t^2 + \dots]. \quad (2.32)$$

Equation (2.32) is also obtained by taking the short-time limit of Eq. (2.28a), which is not surprising, since the right-hand side of Eq. (2.28b) can be transformed into that of Eq. (2.28a).

At long times the discrete mode is completely irrelevant, and we obtain a power-law decay for the absorption probability density

$$f_1(\gamma, t) \sim (2\gamma\pi^{1/2})^{-1} t^{-3/2} \quad (2.33)$$

($t \gg \gamma^{-2}|\gamma - 1|$). As a consequence of the stronger absorption, the onset of the asymptotic regime occurs earlier for large values of γ (for which we must simply require $\gamma t \gg 1$). A useful form of the solution for large values of γ is obtained by a truncation of the series in Eq. (2.28b). The series converges fast: keeping only the first two terms gives a margin of error already lower than 10% (at any time) if $\gamma = 3$ and lower than 3% if $\gamma = 5$.

The analogy with the problem of the linear harmonic chain with a lighter isotopic impurity comes immediately to mind. There we also have a composite eigenvalue spectrum formed by a continuum and an isolated point, which correspond, respectively, to the extended states and the single localized state. The relation between the random walk and the problem of lattice vibrations was explored long ago by Teramoto.^{21,22}

Problems related to those discussed in this section also appear in the area of chemical kinetics.^{18,23} Ninham, Nossal, and Zwanzig solved a system of rate equations,²³ which was later used in the study of the helix-random-coil transformation.²⁴ They showed that, when the value of a parameter increases beyond a certain threshold, two discrete eigenvalues occur outside the continuum (one of them is always present, corresponding to the equilibrium solution).

III. MANY-DEFECT KINETICS

Let us now assume that there is a distribution of noninteracting random walkers in the lattice. When any of these walkers reaches the site $s=1$, it may be absorbed with a probability γ . Once one of the walkers has "gone into limbo," we consider the process as terminated. In this way we can describe molecular relaxation by diffusing defects, as in the Glarum model. We will be also able to investigate (in Sec. IV) the distribution of closed times in ionic channels, assuming that the channel opening is mediated by diffusing defects.

Since the walkers are independent, the probability that a walker starting from site s at $t=0$ is at n at t is still given by the solution to the master Eq. (2.1). It is relatively simple to compute the probability $\Phi(\gamma, t)$ that all the walkers survive at time t .^{15,25} If the absorption of a walker is identified with the relaxation (or annihilation) of a target, then we can evaluate the average target-relaxation rate as

$$f(\gamma, t) = - \frac{\partial \Phi(\gamma, t)}{\partial t}. \quad (3.1)$$

We can also think of $f(\gamma, t)$ as the distribution of target survival times for an ensemble of systems.

Following Tachiya²⁵ we consider N walkers on a V -site lattice. Hence

$$\Phi(\gamma, t) = \sum_{s_1=1}^V \dots \sum_{s_N=1}^V \prod_{i=1}^N P_{s_i}(\gamma, t) u(s_1, \dots, s_N). \quad (3.2)$$

Here, $u(s_1, \dots, s_N)$ describes the initial distribution of the walkers. If, for example, we choose the walkers to be distributed forming a regular array or superlattice with a uniform separation b , then

$$u(s_1, \dots, s_N) = \prod_{i=1}^N \delta_{s_i, ib}, \quad (3.3)$$

and

$$\Phi(\gamma, t) = \prod_{i=1}^N P_{ib}(t). \quad (3.4)$$

This result is quite obvious. The probability for a simultaneous survival of the N walkers is the product of the survival probabilities for each of the walkers.

More interesting for us is the case when the N walkers are randomly distributed over the lattice, with a density $c = N/V$. Then,

$$u(s_1, \dots, s_N) = V^{-N}, \quad (3.5)$$

and

$$\begin{aligned} \Phi(\gamma, c; t) &= \left[1 - \frac{c}{N} \sum_{s=1}^V P_s^*(\gamma, t) \right]^N \\ &= \exp[-cQ(\gamma, t)], \end{aligned} \quad (3.6)$$

where P_s^* is given by Eq. (2.2) and

$$Q(\gamma, t) = \sum_{s=1}^{\infty} P_s^*(\gamma, t). \quad (3.7)$$

The last line in Eq. (3.6) is obtained if we take the $V \rightarrow \infty$ limit.

The meaning of the function Q can be understood if we consider the following auxiliary problem: Suppose that it is known that one walker started from each lattice site at $t=0$. The walkers are then allowed to jump into the limbo state without interrupting the process when one of them is absorbed. Under these conditions, $Q(\gamma, t)$ can be thought of as the total limbo population, and its time derivative $Q'(\gamma, t)$ gives the walker flux into the limbo state. Using Eq. (3.1), we have for the target relaxation rate,

$$f(\gamma, t) = cQ'(\gamma, t) \exp[-cQ(\gamma, t)]. \quad (3.8)$$

The distribution (3.5) leads to a form of the target-annihilation problem in which the target is not necessarily annihilated when reached by a defect. When $\gamma=1$, we obtain Bordewijk's form of the Glarum model (except for a factor of 2 arising from our consideration of a semi-infinite lattice instead of an infinite one.) We note that, in the context of viscous liquids, a natural generalization of the Glarum model to arbitrary relaxation rates would require the explicit consideration of an infinite lattice. The reason for this is that the defects should be allowed to move through the target without relaxing it. In our formulation, motivated by the membrane-channel problem, the defects may come only from one side of the target. The solution to the infinite-lattice problem can also be obtained with the methods used here.

The evaluation of $Q(\gamma, t)$ involves a double summation, over sites and walkers. However, it is not difficult to show that

$$Q'(\gamma, t) = \gamma P_1(\gamma, t). \quad (3.9)$$

In order to prove Eq. (3.9), note first the relation

$$p_{ns}(\gamma, t) = p_{sn}(\gamma, t), \quad (3.10)$$

which expresses the "reversal symmetry" for the probability along each path connecting any two sites. Equation (3.10) leads to

$$\sum_{s=1}^V p_{1s}(\gamma, t) = \sum_{n=1}^V p_{n1}(\gamma, t). \quad (3.11)$$

Taking into account the remark following Eq. (3.7), we can write

$$Q'(\gamma, t) = \gamma \bar{P}(\gamma, t), \quad (3.12)$$

where

$$\bar{P}(\gamma, t) = \sum_{s=1}^V p_{1s}(\gamma, t) \quad (3.13)$$

gives the total population of site $s=1$. Using Eq. (3.11), Eq. (3.9) follows. The derivative Q' is then given directly by the one-walker equation (2.25).

Using the initial condition $Q(\gamma, 0) = 0$, and Eqs. (2.25) and (3.12), we obtain the following expression for $Q(\gamma, t)$:

$$Q(\gamma, t) = \frac{\gamma^2}{2\pi} \int_0^\pi dq \frac{(1 + \cos q)}{(1 - \cos q)} h(q) (1 - e^{-2t(1 - \cos q)}) - \frac{\gamma - 2}{\gamma} \bar{g}(t) \theta(\gamma - 2), \quad (3.14)$$

with $\bar{g}(t) = g(t) - 1$. In the special cases $\gamma=1$ and $\gamma=2$ we find

$$Q(1, t) = 2te^{-2t}[I_0(2t) + I_1(2t)] - \frac{1}{2} + \frac{1}{2}e^{-2t}I_0(2t), \quad (3.15)$$

and

$$Q(2, t) = 2te^{-2t}[I_0(2t) + I_1(2t)], \quad (3.16)$$

respectively. The expression for $Q'(1, t)$ was found by Helman and Funabashi in their study on electron scavenging and ion recombination in liquids.²⁶

A power expansion of Eq. (3.14) leads to the following short-time approximation:

$$Q(\gamma, t) = \gamma t - \frac{\gamma^2 t^2}{2} + \dots \quad (3.17)$$

Therefore, the distribution of survival times begins as

$$f(\gamma, c; t \ll \gamma^{-1}) \cong c\gamma[1 - \gamma(1 + c)t]. \quad (3.18)$$

Of course, we can calculate $Q(t)$ by explicit summation instead of using Eq. (3.9). In this manner, we can express $Q(t)$ in terms of Bessel functions in the cases $\gamma \gg 1$ and $|\gamma - 1| \ll 1$. This route is also appropriate to obtain a long-time approximation. The computations are tedious but straightforward. Aside from the recursion relation, the following formulas are useful:

$$e^{-x} \left[I_0(x) + 2 \sum_{j=1}^{\infty} I_j(x) \right] = 1 \quad (3.19)$$

and

$$\begin{aligned} \sum_{j=1}^{\infty} \sum_{i=j}^{\infty} I_i(x) &= \sum_{j=1}^{\infty} j I_j(x) \\ &= (x/2)[I_0(x) + I_1(x)]. \end{aligned} \quad (3.20)$$

If $\gamma \gg 1$, we get

$$\begin{aligned} Q(\gamma \gg 1, t) &\cong Q(1, t) + 1 \\ &\quad - \gamma^{-1} \{1 + e^{-2t}[I_0(2t) + I_1(2t)]\} \\ &\quad - \gamma^{-1}(\gamma - 2)g(t) \\ &\quad + \gamma^{-2}e^{-2t}[I_1(2t) + I_2(2t)]. \end{aligned} \quad (3.21)$$

In particular,

$$Q(\infty, t) = Q(1, t) + 1, \quad (3.22)$$

which is as it should be, since when $\gamma = \infty$ and $t > 0$ the flux into limbo is controlled by the rate of the jump from site $s=2$ to site $s=1$. This is also the reason why the "instantaneous relaxation" assumed in the usual formulation of the Glarum model corresponds to $\gamma=1$ in this work. The full expression for $f(\gamma, c; t)$ when $\gamma \gg 1$ is given in the Appendix.

The long-time behavior of $Q(\gamma, t)$ is given by

$$Q(\gamma, t) \cong \frac{2t^{1/2}}{\pi^{1/2}} + \frac{1}{2} - \frac{1}{\gamma} + \left[\frac{1}{8} - \frac{1}{\gamma} + \frac{1}{\gamma^2} \right] \frac{1}{(\pi t)^{1/2}}. \quad (3.23)$$

To obtain this result we note that, because of the $\exp[-2t(1-\cos q)]$ factor in the relevant integrands, only the “long-wavelength” (small- q) modes contribute at long times. The approximations $\gamma^2 t \gg |\gamma - 1|$ and $t \gg 1$ are then made.

The leading term in Eq. (3.23) gives the “stretched exponential” form of $\Phi(\gamma, c; t)$. It corresponds to Bordewijk’s solution of the Glarum model on a continuum.¹¹ As noted by Blumen and co-workers,²⁷ the $t^{1/2}$ stretched exponential should be a general feature of this type of models. This term is also independent of γ , which means that it corresponds to processes controlled by the walk dynamics and not by the relaxation at the target. It is due to the contribution of walkers originally located at distances of the order of $t^{1/2}$ from the target.

The following term in Eq. (3.23) becomes important at small values of γ , for which there will be on the average many passages of the walkers through site $s=1$ before the target is relaxed. For small values of γ , a long time must elapse before the Bordewijk asymptotic form takes over.

The function $Q(\gamma, t)$ is shown in Figs. 6 and 7 using linear and logarithmic scales, respectively. $Q(\infty, 0) = 1$ because a defect at $s=1$ is instantaneously relaxed. The linear (if $\gamma < \infty$) and $t^{1/2}$ regimes are clearly visible in Fig. 7; the crossover between both regimes is smoother for small values of γ .

The distribution $f(\gamma, c; t)$ of target survival times is presented in Fig. 8 for the values of γ specified in Figs. 6 and 7. We have chosen the defect concentration to be $c=0.1$. The initial value is seen to be $f(t=0) = 0.1\gamma$, in agreement with Eq. (3.18). Since the target will relax at $t < \infty$ for any positive values of γ and c , and since it can relax only once, the time integral of $f(\gamma, c; t)$ must always be equal to one. The long-time form of $f(\gamma, c; t)$ can be obtained from Eqs. (3.8) and (3.23):

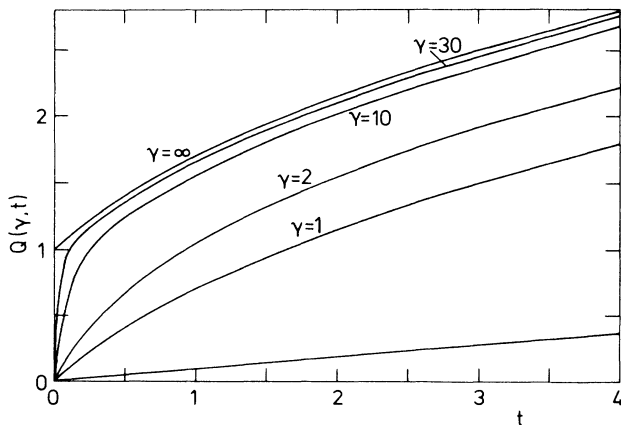


FIG. 6. Exponent in the target survival probability divided by the initial walker concentration c . Curves for various values of the absorption rate are shown.

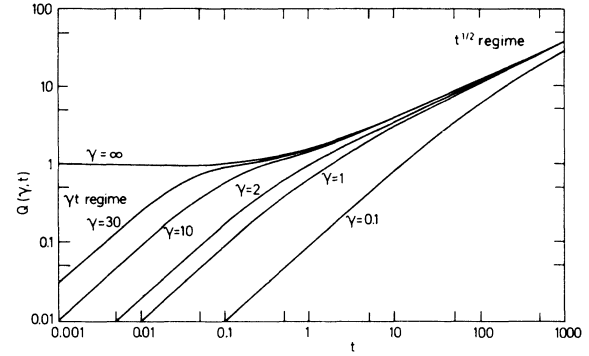


FIG. 7. Same as in Fig. 6, but on a logarithmic scale that makes the various regimes evident.

$$f(\gamma, c; t) \rightarrow c(\pi t)^{-1/2} \exp(-2ct^{1/2}/\pi^{1/2}). \quad (3.24)$$

Due to the reasons discussed above, the dependence on γ disappears if we wait long enough. This can be seen in Fig. 8. An interesting feature of this figure is the quite abrupt change in the slope that occurs in the $\gamma > 10$ curves. The faster decay at short times is contributed by those configurations in which a defect is originally at $s=1$. Once this defect has moved away from $s=1$ without annihilating the target, the system enters into a slower-decay regime in which no defects are privileged. Note that, while the relative height of the short-time feature must depend on the number of configurations in which there is a walker at site $s=1$ and $t=0$, and thus on c , the time at which the crossover occurs is independent of the defect concentration. Compare with Fig. 10, in which we start with the certainty that there is a defect at $s=1$ and $t=0$.

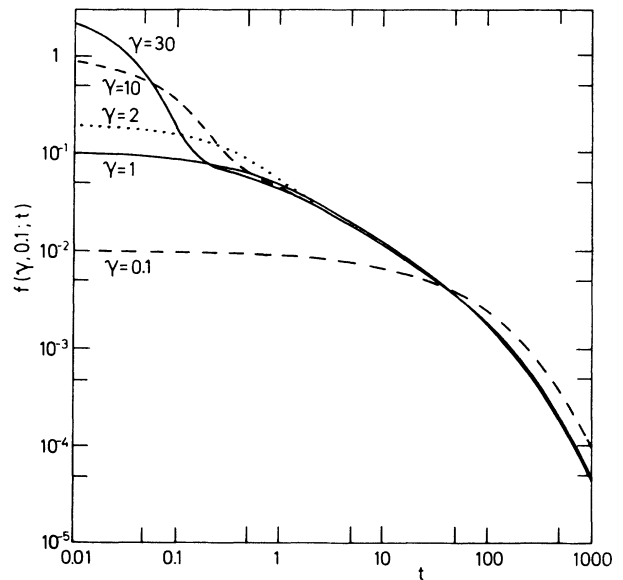


FIG. 8. Distribution of target survival times given a concentration $c=0.1$ of walkers for the absorption rates of Figs. 6 and 7.

IV. CLOSED-TIME DISTRIBUTIONS OF IONIC CHANNELS IN MEMBRANES

A. The defect-diffusion model

The predictions of the defect-diffusion model conceived by Lauger⁸ are borne out by the experimental data on a collection of channels.^{8,9} Lauger assumed that the channel is closed by a molecular group moving from the channel wall into the ionic pathway. This movement leaves behind a defect, which can be interpreted as a “free volume” in the channel wall. The defect is then allowed to perform a random walk inside the close-packed protein. Upon returning to its original position at the wall, it can either induce the reopening of the channel or continue its walk. In more general terms, the idea is that the molecular group can return from its position in the ionic pathway to the channel wall only when the channel wall is exactly in the same state it was when the molecular group “swung away.” The processes in which the channel wall makes a transition from the original state to other states and back are modelled by the diffusion of defects in the protein molecule.

Lauger made a simulation of the random walk on a finite 3D lattice, obtaining good agreement with experimental data for the rabbit corneal endothelium channel⁶ and the frog end-plate channel.²⁸ This good agreement and the physical appeal of the model motivated us to search for an analytical solution. This solution is relatively easy to obtain if we constrain the defect motion to a semi-infinite chain. Before giving the mathematical formulation, let us make some comments on the nature and scope of the model we are considering.

(1) An argument in support of the one-dimensional model is that the chain structure of the protein molecule may render the defect diffusion very anisotropic, favoring one-dimensional motion along the main chain.

(2) Since the protein is a finite structure, only a limited (although probably large) number of sites is available for the walk. For an M -site lattice, finite-size effects become important at times of the order of M^2 . In Ref. 9 we estimated that the number of sites that effectively participated in the diffusion process in the corneal endothelium⁶ and rat colonic²⁹ channels was of the order of 10. The estimate for the end-plate channel²⁸ indicated that about 50 sites must have participated. Hence, it appears that in the time scales probed by the experiments only a very small fraction of the protein sites is involved; we may then assume that the finiteness of the protein is not really relevant to the process discussed here.

(3) In its original version,⁸ Lauger’s model is a single-defect model. As such, its solution in the one-dimensional configuration is given by the formulas of Sec. II B. Here we consider the possibility that there are other defects (besides the one that originates at the channel wall) in the protein at the time the channel closes. Each of these defects can reopen the channel upon arrival to the “original” wall site from which the blocking group swung. The evaluation of this contribution is related to the many-defect model discussed in Sec. III.

(4) All the defects are considered to be identical and

noninteracting. This last assumption, which is crucial if we want analytical solutions, may also be the most reasonable one if the defects are indeed free volumes.

(5) The distribution of open times is usually simpler than that of closed times. In Lauger’s picture,⁸ the channel closing is described by a rate γ' associated with the displacement of the blocking group into the channel. We will not consider explicitly the closing process in what follows.

(6) We assume the temporal boundary between closed and open states to be punctual. This agrees with the observation that the current is not seen to increase or decrease smoothly between conducting and nonconducting states. The displacement of the blocking defect is too fast to be detected on the experimental time scales.

B. Model formulation

The defect motion takes place on the lattice shown in Fig. 1. The site $s=1$ corresponds to the location at the pore wall where a defect, the “Lauger” defect, is created at $t=0$ by the channel-blocking displacement; the channel is assumed to close instantaneously at $t=0$. In the rest of the lattice ($s > 1$) we add a random distribution of defects (the “Glarum” defects) with a specified concentration c . Any of the defects can reopen the channel upon arrival at site $s=1$.

Inside the protein the defects are assumed to diffuse with a constant hopping rate Γ . It is convenient to formulate the model using a time scale for which this rate is unity. The relation between the usual, “experimental,” time t_{expt} (measured in seconds) and the dimensionless scaled time t is then

$$t = \Gamma t_{\text{expt}} . \quad (4.1)$$

The scaled rate at which a closed channel is reopened by a defect $s=1$ will be denoted by γ . (This corresponds to the walker absorption rate at the boundary in Secs. II and III.) A defect that reopens the channel can be thought of as jumping into the limbo state L . When one of the defects goes into L , the channel reopens instantaneously and the process is considered terminated. With our definitions, the single-defect kinetics is described by the master Eq. (2.1) for the continuous-time random walk.

The probability $\Phi(\gamma, c; t)$ of simultaneous survival of all the walkers can now be identified with the probability that the channel is still closed at time t . The function $f(\gamma, c; t)$ is then the probability density that the “waiting time” for the reopening of the channel has a length t . It should be noted that on the usual time scale of t_{expt} the probability density is obtained by multiplying f by the defect hopping rate, i.e.,

$$f_{\text{expt}}(\gamma, c; t_{\text{expt}}) = \Gamma f(\gamma, c; t) . \quad (4.2)$$

The distribution $f_{\text{expt}}(t_{\text{expt}})$ of closed times is the magnitude directly observed in the experiments.

The infinite one-dimensional and the finite three-dimensional models have an important feature in common: In both cases the Lauger defect must return to the origin. Hence, the channel will be reopened at $t < \infty$ for any $\gamma > 0$, even in the absence of Glarum defects. This is

expressed through the equation

$$\int_0^\infty f(\gamma, c; t) dt = 1. \tag{4.3}$$

Note that in an infinite three-dimensional lattice the Luger defect can migrate to infinity, and thus Eq. (4.3) can be valid only for $c > 0$.

Since the site $s=1$ is known to be occupied by a defect at $t=0$, then the initial value of f is given by

$$f(\gamma, c; 0) = \gamma, \tag{4.4a}$$

or

$$f_{\text{expt}}(\gamma, c; 0) = \gamma \Gamma \equiv \gamma_{\text{expt}}. \tag{4.4b}$$

It is clear that γ_{expt} is the rate for channel deblocking measured in units of t_{expt} .

C. Solution

The probability $\Phi(\gamma, c; t)$ that a channel that closed at

$t=0$ is still closed at time t can be calculated as in Sec. III. We find

$$\Phi(\gamma, c; t) = P_1(\gamma, t) \exp \left[-c \sum_{s=2}^\infty P_s^*(\gamma, t) \right]. \tag{4.5}$$

This yields the following form for the distribution of closed times:

$$f(\gamma, c; t) = \{ c P_1(t) [P_1'(t) + \gamma P_1(t)] - P_1'(t) \} \times \exp \{ c [1 - P_1(t) - Q(t)] \}. \tag{4.6}$$

Here P_1 gives the survival probability of Luger's defect (i.e., the probability that it has not reopened the channel), P_1' is its time derivative, and Q is defined by Eq. (3.7). These functions depend on γ but not on c .

In Secs. II and III we have obtained all the functions needed to evaluate Eq. (4.6). Let us now summarize some of the results that can be expressed in terms of Bessel functions. The argument of I_0 and I_1 is always $2t$,

$$f(1, c; t) = e^{-2t} \{ t^{-1} I_1 + c e^{-2t} [(I_0 + I_1)^2 - t^{-1} I_1 (I_0 + I_1)] \} \exp \{ c \{ \frac{3}{2} - e^{-2t} [(\frac{3}{2} + 2t) I_0 + (1 + 2t) I_1] \} \}, \tag{4.7}$$

$$f(2, c; t) = 2e^{-2t} (I_0 - I_1 + c e^{-2t} I_0 I_1) \exp \{ c [1 - e^{-2t} (I_0 + 2t I_0 + 2t I_1)] \}, \tag{4.8}$$

$$f(\gamma \gg 1, 0; t) = \frac{e^{-2t}}{\gamma t} \left\{ -\frac{2}{\gamma} I_0(2t) + \left[1 + \frac{2}{\gamma} \left(1 + \frac{1}{t} \right) \right] I_1(2t) \right\} + \left[\gamma - \frac{1}{\gamma} - \frac{2}{\gamma^2} \right] \exp [-\gamma^2 t / (\gamma - 1)]. \tag{4.9}$$

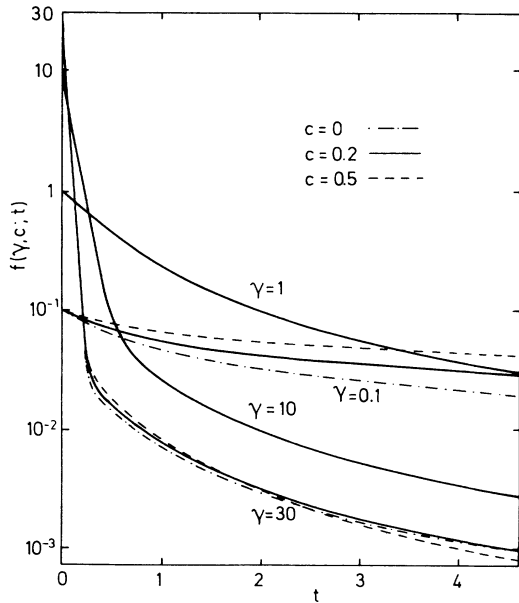


FIG. 9. Closed-time distribution as a function of time for several values of the parameters γ (rate constant for channel reopening) and c (density of Glarum defects). Note the well-defined short-time exponential decay in the $\gamma=10$ and $\gamma=30$ curves.

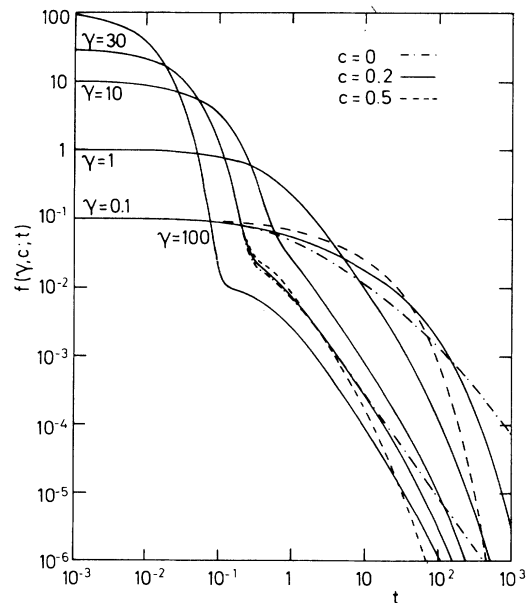


FIG. 10. Closed-time distribution on a log-log scale. The different regimes can be observed. The long-time behavior is given either by a power law ($c=0$) or by a stretched exponential ($c>0$).

The solution $f(\gamma \gg 1, c; t)$ for arbitrary values of c is given in the Appendix.

The appearance of the factor $\exp(-2t)$ multiplying each of the Bessel functions is characteristic of the solutions to the model under consideration. The Glarum defects contribute the elements containing the factor c in Eqs. (4.7) and (4.8). Setting $c=0$ we are left with the contribution of Lauger's defect. The isolated solution $\tilde{\phi}$ does not contribute to Eqs. (4.7) and (4.8). In the $\gamma \gg 1$ case, however, its contribution at $t < \gamma^{-1}$ is much larger than that of all the continuum states taken together, being of the order of γ at $t=0$. This "surface-state" contribution

is expressed through the last term in Eq. (4.9). Therefore, if $\gamma \gg 1$, we have initially a well-defined exponential decay. This behavior is clearly seen in the curves for $\gamma=10$ and $\gamma=30$ in Fig. 9, where we have plotted the closed-time distribution for several values of γ and c . In the $\gamma=30$ case, the closed-time distribution is seen to decay by three orders of magnitude as essentially a pure exponential.

The long-time form of $f(\gamma, c; t)$ is obtained using the same approximations ($\gamma^2 t \gg |\gamma-1|, t \gg 1$) that led to Eq. (3.23). We find

$$f(\gamma, c; t) = \left[\frac{c}{\pi\gamma t} + \frac{1}{2\gamma\pi^{1/2}t^{3/2}} \right] \exp \left\{ c \left[-\frac{2t^{1/2}}{\pi^{1/2}} + \frac{1}{2} + \frac{1}{\gamma} - \left(\frac{1}{8} + \frac{1}{\gamma^2} \right) \frac{1}{(\pi t)^{1/2}} \right] \right\}. \quad (4.10)$$

The discussion following Eq. (3.23) also applies to the exponent in Eq. (4.10). The $t^{-3/2}$ term in the prefactor is the contribution of Lauger's defect, and corresponds to the single-walker result, Eq. (2.33). The proportionality with γ^{-1} is reasonable, since for large γ there is an enhanced probability of early channel opening. Due to the normalization condition, Eq. (4.3), this reduces the chance of having long closed periods. On the other hand, the c -dependent term in the prefactor is proportional to t^{-1} , not to $t^{-1/2}$ as in the "uniform background" model [cf. Eq. (3.24)]. This is due to the exclusion of site $s=1$ from the domain where the Glarum defects are distributed at $t=0$.

In Fig. 10 we show $f(\gamma, c; t)$ on a log-log scale, which allows us to follow its behavior over several time decades. In the large- γ curves a shoulder appears beyond the exponential region; this shoulder, whose origin was discussed at the end of Sec. III, becomes more marked with increasing γ . The Lauger-dominated, $f(\gamma, 0; t) \sim t^{-3/2}$, and Glarum-dominated, $f(\gamma, c \neq 0; t) \sim \exp(-ct^{1/2})$, asymptotic regimes become evident at long times.

V. DISCUSSION

A. The experimental data

There are some details that must be borne in mind when fitting theoretical predictions to a set of data. Owing to the finite experimental resolution, the briefest closed events will in general go undetected. Therefore, the total number of closed events n must be taken as an adjustable parameter; this permits a vertical shift of the predicted curve without changing its shape.

The data for six channels were analyzed in some detail in Ref. 9. These six sets of data may be divided into two groups. In the fact group (group I) it appears that the experiments were performed over a time range corresponding to an intermediate stage in the evolution of $f(t)$; consequently, it is possible to estimate the magnitude of the various parameters involved. This group includes the rabbit corneal endothelium,⁶ the frog end-plate,²⁸ and the

rat colonic²⁹ channels. In the three cases we find $\gamma \geq 2$.

The second group (group II) is characterized by a power-law dependence of $f(t)$: $f(t) \sim t^{-x}$, with $x \sim 1.5$. This seems to indicate that the experimentalist has recorded data corresponding to the long-time tail of the distribution for a Lauger defect. Because only the long-time tail has been observed, it is not possible to evaluate separately the different parameters. But we can certainly conclude that the hopping rate Γ is higher than for the proteins in group I. The gramicidin A,³⁰ rat skeletal muscle,³¹ and NG108-15 neuroblastoma x glioma³² channels belong in this class of channels with fast hopping rates.

In Figs. 11 and 12 we show two typical sets of data, one belonging in each group. The data of Liebovitch *et al.*⁶ for the rabbit corneal endothelium channel (group I) are displayed in Fig. 11, together with the results of

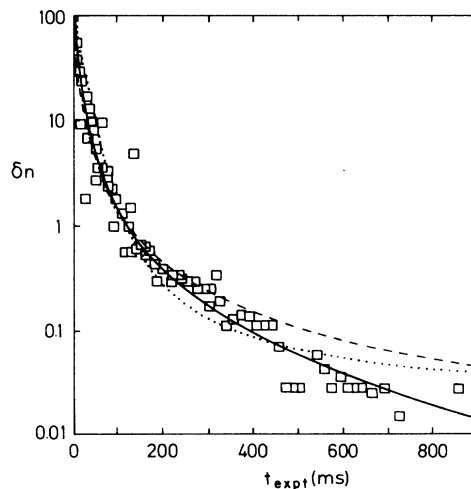


FIG. 11. Closed-time distribution for a channel in the rabbit corneal endothelium. $\delta n = n\Gamma f(t) \times 10^{-3}$ s. The experimental data (squares) of Liebovitch *et al.* (Ref. 6) are plotted together with the results of Lauger's simulation (Ref. 8) (\cdots) and our own results for $\gamma=2, c=0.5$ (—) and $\gamma=2, c=0$ (---). We took $\Gamma=32 \text{ s}^{-1}$ and $n=1560$.

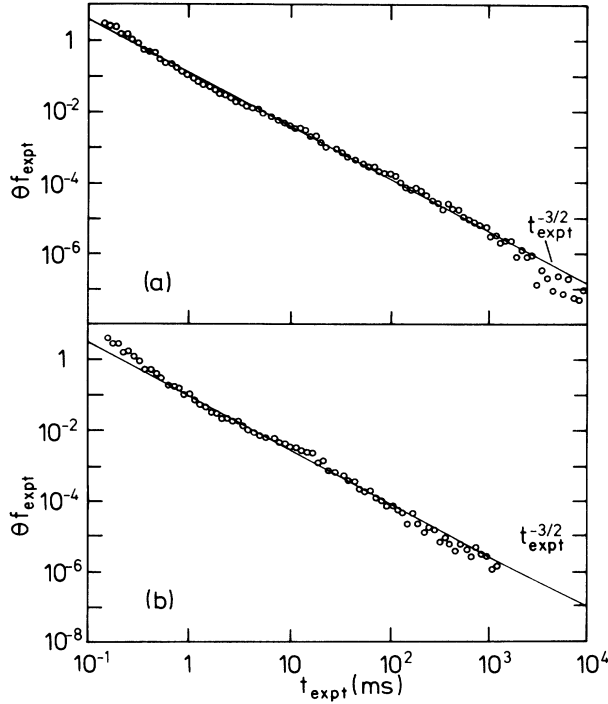


FIG. 12. Closed-time distribution for the K^+ channel in NG108-15 cells. The experimental data (circles) of McGee *et al.* (Ref. 32) are plotted for the “control” (a) and “enriched” (b) patches. The enrichment was due to the addition of arachidonic acid. The straight lines have a slope of $-\frac{3}{2}$. The constant Θ is proportional to the product $n\gamma\Gamma$.

Läuger’s simulation and of our calculation. Läuger allowed the defect to perform a random walk on a cube containing 125 sites; he took $\gamma=33$ and $\Gamma=\frac{12}{11}\text{ s}^{-1}$. We choose $\gamma=2$ and $\Gamma=32\text{ s}^{-1}$. The value we estimate for the total number of closed events (detected and undetected) is $n=1560$, not much higher than the number of events actually recorded (1465). There is a certain flexibility in the determination of γ and c . In the figure we have taken two extreme values, $c=0$ and $c=0.5$, for the concentration of Glarum defects. We can see that the agreement is excellent for $\gamma=2$ and $c=0.5$. If we decrease c , a good fit is still obtained by increasing the value of γ . However, c cannot be too small if we want to reproduce the “downward slant” apparent at the longest times.

The K^+ channel in NG108-15 cells studied by McGee and coworkers³² is a good example of the second group of channels. In Fig. 12 we show the data for “control” and “enriched” (with arachidonic acid) patches. Although the data were originally fit using a superposition of six exponentials, we can see from Fig. 12(a) that $f(t)\sim t^{-3/2}$ gives a nearly perfect fit to the data from the “control” patches over almost four orders of magnitude in the time. At the longest times ($t_{\text{expt}} > 1\text{ s}$) the data points lie below the $t^{-3/2}$ line. This would be consistent with the presence of a low concentration of Glarum defects, which become asymptotically dominant.

For the enriched patches there is a gentle oscillation superimposed on the $t^{-3/2}$ line. While the Läuger defect

diffusion still plays the main role, the enrichment seems to be responsible for the onset of a second, much weaker, process that generates the observed fluctuations.

B. Other formulations

As mentioned in the Introduction, Liebovitch *et al.*⁶ obtained a good fit to their data on the corneal endothelium channel using the stretched exponential form for $f(t)$. A discrimination between their description and ours would be possible if accurate data at shorter times were available. The reason for this is that, while our f remains finite at $t=0$, in the fractal-related description f increases without limit as $t\rightarrow 0$. For example, while we estimate that about 10^2 brief events went undetected in the corneal endothelium experiment, the formulation of Liebovitch *et al.* leads to the conclusion that about 10^4 brief events were missed.

When the fractal dimension D is close to 2, then the stretched exponential behaves approximately as a power law of the form $f\sim t^{1-D-A}$, where A gives the strength of an effective kinetic rate constant⁶ ($k=At^{1-D}$). In Ref. 6 it was suggested that Ring’s experiment³⁰ could belong in this class. Recently, Liebovitch and Sullivan³³ have analyzed the data of a voltage-dependent K^+ channel from cultured mouse hippocampal neurons using the fractal description. They found that f is approximately given by a power law, with $D\sim 2.07$ and A a function of the applied potential (A decreases with an increment in the magnitude of the applied potential). It is possible that this channel belongs in group II discussed above and that the applied potential distorts the behavior of the defect. However, more analysis is required before arriving at a definitive conclusion.

Although they do not give a random-walk interpretation to their formulation, the assumptions of Millhauser *et al.*⁷ about the Markovian nature of the kinetics and the existence of a large number of states of similar energy in the protein led them to a master equation identical to our Eq. (2.1). Their formulation is then entirely equivalent to that of the one-dimensional Läuger model without the Glarum defects. They also found the asymptotic $t^{-3/2}$ dependence of $f(t)$ and noted that it could describe approximately the data for the gramicidin A³⁰ and rat skeletal muscle³¹ channels. They included the corneal endothelium channel in this group, but we believe it is better described if we include it in our group I as indicated above. On the other hand, these authors made a computer simulation for an M -site linear system, showing that at time $t\sim M^2$ the $t^{-3/2}$ behavior of $f(t)$ is cut off, as it should be expected.

C. Some further comments

It is reasonable to think that the hopping rate Γ and the dimensional deblocking rate $\gamma_{\text{expt}}=\gamma\Gamma$ will depend on the temperature T . Let us see how a change in the temperature would affect the asymptotic form of the closed-time distribution functions for a Läuger defect. From Eqs. (2.33) and (4.2),

$$f_{\text{expt}}(\gamma_{\text{expt}}, 0; t) \simeq \frac{\Gamma^{1/2}}{2\pi^{1/2}\gamma_{\text{expt}}t^{3/2}}. \quad (5.1)$$

If we assume that these rates represent a thermal activation process and write $\Gamma \sim \exp(-W_1/T)$ and $\gamma_{\text{expt}} \sim \exp(-W_2/T)$, we obtain

$$f_{\text{expt}}(\gamma_{\text{expt}}, 0; t) \simeq t_{\text{expt}}^{-3/2} \exp[T^{-1}(W_2 - W_1/2)]. \quad (5.2)$$

In the asymptotic regime and at a given time t_{expt} , f_{expt} will increase or decrease with an increment in T depending on the relative sizes of the activation energies for the hopping and deblocking processes. The bigger the difference between W_2 and $W_1/2$, the more sensitive the result to changes in the temperature.

One of the motivations behind our work—and also, we believe, that of Refs. 6, 7, and 8—has been the desire to get rid of the parameter proliferation that is often needed if one insists in fitting the data with a superposition of exponentials. Without abandoning this simplifying philosophy, we note that reality may be more complicated than our ideal random walk would suggest; additional parameters may be necessary to describe the behavior of some channels. In particular, it would be interesting to consider the effect of adding internal states to some of the sites visited by the defect.³⁴ These internal states may be specially useful if we try to describe the effects of structural inhomogeneities in the chain. They might account for “anomalously” high values of $f(t)$ at long times. A possible case in point could be the suberyldicholine-activated frog end-plate channel²⁸ whose longest-time data give an $f(t)$ much higher than what is predicted by the one-dimensional defect-diffusion model.⁹ (Alternative explanations are possible:^{8,9} The system may not be truly one dimensional, or there may be a second, much slower channel present.)

D. Concluding remarks

In this paper we have presented the solution to a defect-diffusion model for the gating of ionic channels in cell membranes. Along the way, we have also solved exactly a model related to that of Glarum for molecular relaxation. Our solution is valid for arbitrary values of the relaxation rate and the time.

The diversity of the ionic channels existing in nature is huge. We expect that the model presented here will be helpful to our understanding of the processes occurring in a large subset of the channels. The analyzed evidence seems to support this expectation.

Many external factors, like the temperature, agonist nature and concentration, applied potential, etc., may affect the channel kinetics. In the model discussed here, these factors can influence the measured closed-time distribution only through their effect on the parameters γ , c , and Γ . The sensitivity of the distribution to changes in γ was explored in Ref. 9, where we also estimated the dependence of γ on the nature of the agonist for the frog end-plate channel studied by Colquhoun and Sakmann.²⁸

ACKNOWLEDGMENTS

It is a pleasure to thank P. Lauger for his continuous encouragement and for many fruitful discussions. I am

also grateful to J. Jackle for reading the manuscript and making useful suggestions. This research was supported by the Sonderforschungsbereich 306 of the Deutsche Forschungsgemeinschaft.

APPENDIX: LARGE- γ RESULTS

Explicit expressions for the probability density $f(t)$ in terms of the Bessel functions $I_0(2t)$ and $I_1(2t)$ can be obtained when $\gamma \gg 1$. We give now the formulas corresponding to the different cases considered in Secs. II–IV. Terms of order γ^{-3} or higher are neglected.

Single defect. Truncation of the series in Eq. (2.28b) yields

$$f_1(\gamma \gg 1, t) = \frac{e^{-2t}}{\gamma t} \left\{ -\frac{2}{\gamma} I_0 + \left[1 + \frac{2}{\gamma} \left(1 + \frac{1}{t} \right) \right] I_1 \right\} + \left[\gamma - \frac{1}{\gamma} - \frac{2}{\gamma^2} \right] g(t), \quad (A1)$$

where $g(t) = \exp[-\gamma^2 t / (\gamma - 1)]$.

Many defects; uniform background case. Equation (3.8) leads to

$$f(\gamma \gg 1, c; t) = c [A_1 + \gamma(\gamma - 2)(\gamma - 1)^{-1} g(t)] \times \exp\{-c [Q(1, t) + 1 + B_1 - (\gamma - 2)\gamma^{-1} g(t)]\}, \quad (A2)$$

with $Q(1, t)$ being given by Eq. (3.15),

$$A_1 = \left[1 - \frac{2}{\gamma^2 t} \right] e^{-2t} I_0 + \left[1 + \frac{1}{\gamma t} + \frac{1}{\gamma^2 t} \left(1 + \frac{2}{t} \right) \right] e^{-2t} I_1, \quad (A3)$$

and

$$B_1 = -\frac{1}{\gamma} [1 + e^{-2t}(I_0 + I_1)] + \frac{1}{\gamma^2} e^{-2t} \left[I_0 + \left(1 - \frac{1}{t} \right) I_1 \right]. \quad (A4)$$

Many defects; ionic channel case. The evaluation of Eq. (4.6) yields

$$f(\gamma \gg 1, c; t) = (A_i + cD_i) \exp(cB_i), \quad (A5)$$

where

$$A_i = \frac{e^{-2t}}{\gamma t} \left\{ -\frac{2I_0}{\gamma} + \left[1 + \frac{2}{\gamma} \left[1 + \frac{1}{t} \right] \right] I_1 \right\} + \frac{\gamma^2(\gamma-2)}{(\gamma-1)^2} g(t), \quad (\text{A6})$$

$$D_i = \frac{e^{-4t}}{\gamma} (I_0 + I_1) \left\{ I_0 + I_1 + \frac{I_1}{\gamma t} \right\} + \frac{\gamma(\gamma-2)e^{-2t}}{(\gamma-1)^2} \left[\left(1 - \frac{2}{\gamma} \right) I_0 + \left(1 - \frac{2}{\gamma} - \frac{2}{\gamma^2 t} \right) I_1 \right] g(t) - \frac{\gamma(\gamma-2)^2}{(\gamma-1)^3} g^2(t), \quad (\text{A7})$$

and

$$B_i = \frac{1}{2} + \frac{1}{\gamma} - e^{-2t} \left\{ \frac{I_0}{2} + 2t(I_0 + I_1) + \frac{1}{\gamma^2} (I_0 + I_1) \right\} - \frac{(\gamma-2)}{\gamma(\gamma-1)} g(t). \quad (\text{A8})$$

The $g(t)$ terms have their origin in the surface state. These large- γ results work well down to values of γ not very far from 2.

-
- ¹B. Hille, *Ionic Channels of Excitable Membranes* (Sinauer, Sunderland, MA, 1984).
- ²*Single Channel Recording*, edited by B. Sakmann and E. Neher (Plenum, New York, 1983).
- ³E. Neher and B. Sakmann, *Nature* (London) **260**, 799 (1976).
- ⁴O. P. Hamill, A. Marty, E. Neher, B. Sakmann, and F. Sigworth, *Pfluegers Arch.* **391**, 85 (1981).
- ⁵D. Colquhoun and A. G. Hawkes, *Proc. R. Soc. London Ser. B* **211**, 205 (1981).
- ⁶L. S. Liebovitch, J. Fischbarg, and J. P. Koniarek, *Math. Biosci.* **84**, 37 (1987).
- ⁷G. L. Millhauser, E. E. Salpeter, and R. E. Oswald, *Proc. Natl. Acad. Sci. U.S.A.* **85**, 1503 (1988).
- ⁸P. Läuger, *Biophys. J.* **53**, 877 (1988).
- ⁹C. A. Condat and J. Jäckle (unpublished).
- ¹⁰S. H. Glarum, *J. Chem. Phys.* **33**, 639 (1960).
- ¹¹P. Bordewijk, *Chem. Phys. Lett.* **32**, 592 (1975).
- ¹²J. Jäckle, *Rep. Prog. Phys.* **49**, 171 (1986).
- ¹³A. Blumen, G. Zumofen, and J. Klafter, *Phys. Rev. B* **30**, 5379 (1984).
- ¹⁴A. Blumen, in *Molecular Dynamics and Relaxation Phenomena in Glasses*, edited by Th. Dorfmueller and G. Williams (Springer, Heidelberg, 1987).
- ¹⁵M. F. Shlesinger and E. W. Montroll, *Proc. Natl. Acad. Sci. U.S.A.* **81**, 1280 (1984).
- ¹⁶G. Williams and D. C. Watts, *Trans. Faraday Soc.* **66**, 80 (1970).
- ¹⁷N. G. van Kampen and I. Oppenheim, *J. Math. Phys.* **13**, 842 (1971).
- ¹⁸N. G. van Kampen, *Stochastic Processes in Physics and Chemistry* (North-Holland, Amsterdam, 1981).
- ¹⁹J. Klíma and L. Skála, *Z. Phys. B* **69**, 97 (1987).
- ²⁰M. Schwarz, Jr., and D. Poland, *J. Chem. Phys.* **63**, 557 (1975).
- ²¹E. Teramoto, *Prog. Theor. Phys.* **24**, 1296 (1960).
- ²²M. N. Barber and B. W. Ninham, *Random and Restricted Walks* (Gordon and Breach, New York, 1970).
- ²³B. Ninham, R. Nossal, and R. Zwanzig, *J. Chem. Phys.* **51**, 5028 (1969).
- ²⁴J. A. Ferretti, B. W. Ninham, and V. A. Parsegian, *Macromolecules* **3**, 34 (1970).
- ²⁵M. Tachiya, *Radiat. Phys. Chem.* **17**, 447 (1981).
- ²⁶W. P. Helman and K. Funabashi, *J. Chem. Phys.* **66**, 5790 (1977).
- ²⁷A. Blumen, I. Klafter, and G. Zumofen, in *Optical Spectroscopy of Glasses*, edited by I. Zschokke (Reidel, Dordrecht, 1986).
- ²⁸D. Colquhoun and B. Sakmann, *J. Physiol. (London)* **369**, 501 (1985).
- ²⁹R. Reinhardt, R. J. Bridges, W. Rummel, and B. Lindemann, *J. Membr. Biol.* **95**, 47 (1987).
- ³⁰A. Ring, *Biochim. Biophys. Acta* **856**, 646 (1986).
- ³¹A. L. Blatz and K. L. Magleby, *J. Physiol. (London)* **378**, 141 (1986).
- ³²R. McGee, Jr., M. S. P. Sansom, and P. N. R. Usherwood, *J. Memb. Biol.* **102**, 21 (1988).
- ³³L. S. Liebovitch and J. M. Sullivan, *Biophys. J.* **52**, 979 (1987).
- ³⁴See, for example, J. W. Haus and K. W. Kehr, *Phys. Rep.* **150**, 263 (1987).